Surface Segregation in Polymer Blends Driven by Surface Freezing

Shishir Prasad, Laurie Hanne, and Ali Dhinojwala*

Department of Polymer Science, The University of Akron, Akron, Ohio 44325-3909

Received June 7, 2006
Revised Manuscript Received August 8, 2006

Acrylate polymers with hydrophobic side chains exhibit surface freezing, where a monolayer of ordered side chains exists on the surface above the bulk melting temperature (T_m).[1−3] Surface freezing is an exception in nature where almost all the materials exhibit the opposite behavior of surface melting.[4] Linear alkanes and alkane analogues are the only other materials that have been shown to exhibit surface freezing.[5,6] For acrylate side chain polymers, the surface order-to-disorder transition ($T_{s,n}$) is first order and takes place 9−20 K above T_m, depending on the length of the side chains (n). In this Communication, we have determined the surface composition and surface ordering temperatures in binary mixtures containing two different lengths of side chains. (We report here the results for $n = 18/22$, and similar results were obtained for $n = 16/18$ and 16/22 blends.) The chemical attachment of alkyl chains to the backbone leads to striking differences from the surface freezing in binary alkane mixtures.[7] Above $T_{s,22}$, the short disordered side chains are preferred on the surface. However, below $T_{s,22}$ the surfaces change discontinuously from a complete miscible to a complete immiscible surface layer. The long ordered side chains completely cover the surface for bulk composition as small as 2 wt %. Below this critical concentration, both the components coexist on the surface in an unmixed state. The surface transition temperatures for the long side chains are insensitive to the bulk concentration. The dependence of $T_{s,22}$ on bulk concentration can be explained by an abrupt increase in the number of side chains/molecule in the ordered state. These results are in contrast to alkanes of similar chain length differences, where the transition temperature is a strong function of composition and remain mixed in the crystal layer.[7]

Surface transition and composition are measured using surface-sensitive infrared−visible sum frequency generation (SFG) spectroscopy and surface tension (γ). SFG involves the spatial and temporal overlap of a high-intensity visible laser beam of frequency ω_{vis} with a tunable infrared beam of frequency ω_{IR}. According to the dipole approximation, the generation of SFG photons [at $(\omega_{vis} + \omega_{IR})$] is forbidden in centrosymmetric bulk and permitted only at interfaces where inversion symmetry is broken. The SFG signal is resonantly enhanced when IR frequency overlaps with the molecular vibrational mode (both IR- and Raman-active modes). Thus, SFG is sensitive to both the composition and orientation of molecules at the interfaces. Further enhancement by 1−2 orders of magnitude in signal is achieved when the angle of input beams is close to the critical angle for total internal reflection (42° with respect to the surface normal was used to probe the polymer−air interface).[8,9] The temperature measurements were done at a heating rate of 0.5 K min^{-1} with a relative accuracy of 0.025 K and an absolute accuracy of 0.5 K. γ was measured using a thin platinum wire of nominal diameter 0.5 mm (the actual diameter was calibrated using heptane) attached to a Wilhelmy Cahn 2000 microbalance.[3] The absolute error in γ is 0.5 mN m^{-1}. The temperature was changed in steps of 0.2 K at 0.1 K min^{-1}, and the data were recorded after 10 min to ensure complete thermal equilibrium.

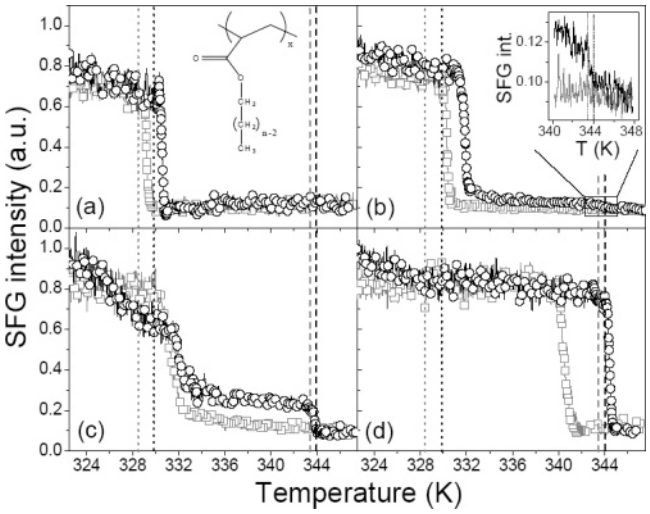

Figure 1. SFG intensity in SSP polarization at 2880 cm^{-1} as a function of temperature for blends with ϕ_b of 0.000023 (a), 0.00023 (b), 0.0023 (c), and 0.023 (d). The (□) and (○) are for cooling and heating cycles, respectively. Also shown are the $T_{s,22}$ (vertical dashed lines) and the $T_{s,18}$ (vertical dotted lines). The black and gray lines are for transition temperature measured for the homopolymers in the heating and cooling cycles. The inset of (a) shows the chemical structure of alkyl side chain acrylate polymer of side chain length "n".

Poly(octadecyl acrylate) (C18: $T_m = 320.7$ K, freezing point (T_f) = 317.2 K, and $T_{s,18} = 329.8$ K) and poly(behenyl acrylate) (C22: $T_m = 336.5$ K, $T_f = 333.5$ K, and $T_{s,22} = 344.0$ K) were prepared using free radical polymerization.[10] The polydispersity (PD) of these polymers was ≈2 and $M_n \approx 15\,000$ g/mol. For γ measurements we have used C18 and C22 from Landec Corp. with PD of ≈10 and $M_n \approx 15\,000$ g/mol prepared using the melt polymerization process. The results were similar for samples prepared using the two techniques. There are two peaks observed in the differential calorimeter measurements at temperatures very close to the transition temperatures of pure C18 and C22, which shows that both C18 and C22 phase separate upon crystallization. Films on sapphire prism for SFG experiments were prepared by solution-casting 6 wt % solution in toluene and subsequently annealed 10 K above $T_{s,22}$ for 4−5 h under vacuum. Blend samples for γ measurements were prepared by mixing the required composition of C18 and C22 in a temperature-controlled glass cell and annealing for a week above $T_{s,22}$.

Figure 1 shows the SFG intensity in SSP polarization (s-polarized SFG, s-polarized visible, and p-polarized IR) at 2880 cm^{-1}, corresponding to the methyl symmetric stretch (r+) as a function of temperature during heating and cooling cycles for blends of C18 and C22. Since the SFG intensity at 2880 cm^{-1} is proportional to the average orientation and the number density of the methyl groups, the sharp drop in SFG intensity indicates an order-to-disorder transition.[1] For concentrations of C22 (ϕ_b is defined in weight fraction and is approximately equal to volume fraction since the densities of C18 and C22 are similar) greater than 2 wt %, we observe only one sharp transition near

* Corresponding author. E-mail: ali4@uakron.edu.

10.1021/ma061266e CCC: $33.50
Published on Web 09/27/2006

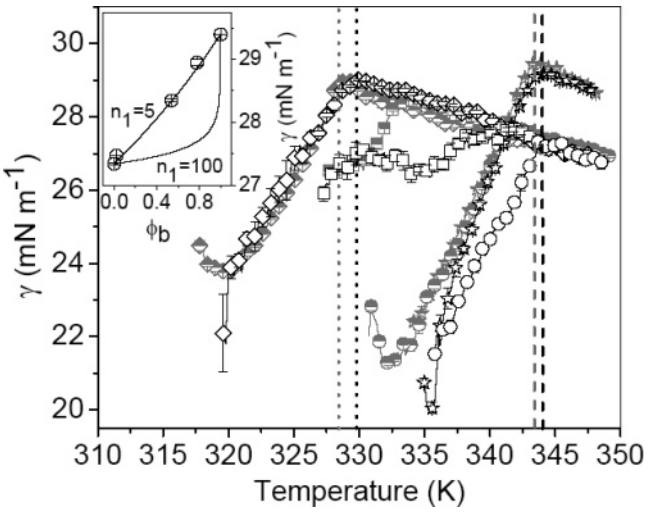

Figure 2. Surface tension as a function of temperature for pure C18 (◇), ϕ_b of 0.00023 (□), 0.023 (○), and pure C22 (★). The half-filled and open symbols are for cooling and heating cycles, respectively. Also shown are the $T_{s,22}$ (vertical dashed lines) and the $T_{s,18}$ (vertical dotted lines). The black and gray lines are used to show the surface transition temperature measured for homopolymers in the heating and cooling cycles, respectively. The inset shows γ at 344 K as a function of ϕ_b. The solid line is a fit using eq 2.

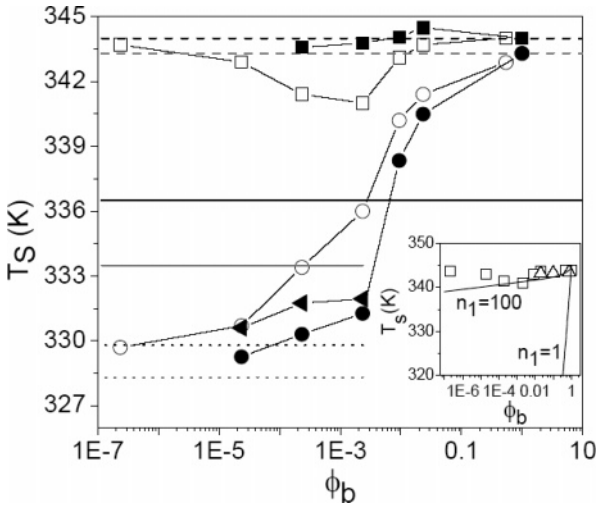

Figure 3. T_s as a function of ϕ_b for cooling (○) and heating (□) cycles. The filled and open symbols represent data obtained from SFG and surface tension, respectively. The filled triangles are the first transition temperatures in the heating run near $T_{s,18}$. At these concentrations, the second transition temperature is near $T_{s,22}$. We are unable to determine the first transition using surface tension due to potential complications associated with crystallization of C22 on the wire below T_m. Shown as horizontal lines (gray: cooling; black: heating) are the $T_{s,22}$ (dashed lines), bulk transition temperatures of pure C22 (T_f and T_m; solid lines), and $T_{s,18}$ (dotted lines). The inset shows the fit for T_s for the C22 phase as a function of ϕ_b using the model discussed in the text. In addition, we have included the T_s for the C16/C22 blend (△).

$T_{s,22}$, indicating that the surfaces are covered with C22 below $T_{s,22}$. Below 2 wt %, we observe two sharp transitions in the heating cycle. This indicates that the C18 and C22 chains are phase separated in the surface ordered state. The first drop in SFG intensity (at lower temperature) is due to the disordering of C18 phase. In this intermediate state there is coexistence of disordered C18 and ordered C22 phases on the surface. At the second transition temperature (at higher temperature) the remaining C22 ordered phase disorder. This is also confirmed by the changes in SFG spectra that will be discussed later. In cooling we observe only one apparent transition temperature with a large undercooling.

γ as a function of temperature shows similar results as SFG (Figure 2). The sharp change in the slope of γ as a function of temperature indicates ordering of surface molecules on top of disordered melt.[3] Above 2 wt % of C22 the transition temperatures are very similar to that of pure C22. The values of γ at 344 K as a function of ϕ_b are shown in the inset of Figure 2. The solid line is a fit using the modified Butlers equation[11] (discussed later). This model also predicts that there is a small surface excess of C18 chains on the surface above $T_{s,22}$. At low values of ϕ_b, the surfaces are covered predominantly with disordered C18 chains above $T_{s,22}$. Below $T_{s,22}$ there is a sharp transition, and the surfaces are completely covered with ordered C22. Below 2 wt % the concentration of C22 on the surfaces decreases with decrease in bulk concentration of C22, eventually resembling that of C18 homopolymer with the transition near $T_{s,18}$.

The transition temperatures determined from γ and SFG data in the cooling and heating cycles are shown in Figure 3. The dotted and dashed lines are the transition temperatures in a heating and cooling cycle of bulk C18 and C22, respectively. The solid lines are T_m and T_f of homopolymer C22. The small differences in the transition temperatures obtained from SFG and γ are not understood. One explanation could be due to sensitivity of the cooling transition to nucleation events, and this may be different for thin films (SFG) and in glass cells (γ). As we decrease the bulk concentration of C22, the hysteresis increases very rapidly due to difficulty in nucleating an ordered

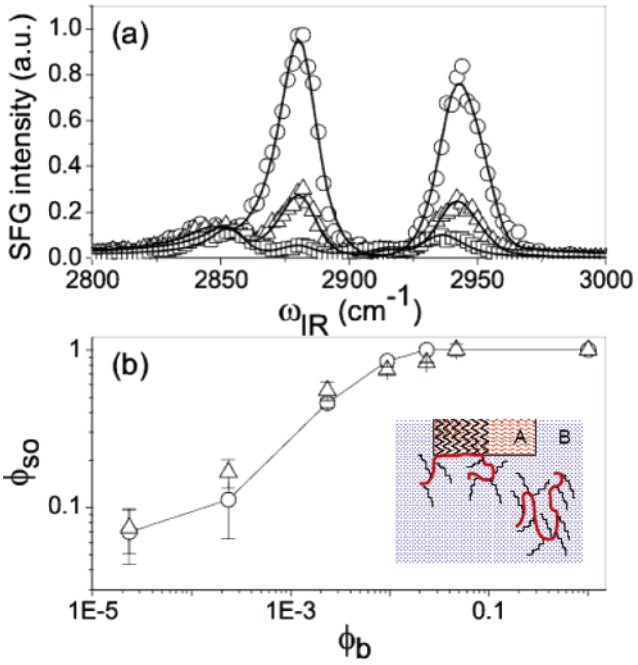

Figure 4. (a) SFG spectra in SSP polarization for $\phi_b = 0.0023$ at 329.5 K (○), 341.3 K (△), and 347.7 K (□). Lines are fits to the spectra using eq 1. (b) ϕ_{so} as a function of ϕ_b for broad (○) and narrower (△) polydisperse samples. The solid line is a guide to the eye. The inset shows a sketch of the ordered C22 phase (A) on the surface coexisting with disordered blend (B). It is not necessary that all the side chains in a molecule get incorporated in the surface layer.

C22 phase. This rapid change in hysteresis coincides with the concentration where the surfaces are no longer completely covered with C22.

To determine the orientation and concentration of the ordered chains on the surface, we measured the SFG spectra at various blend concentrations as a function of temperature. Figure 4a shows the SFG spectra for $\phi_b = 0.0023$ at three temperatures:

below $T_{s,18}$, between $T_{s,18}$ and $T_{s,22}$, and above $T_{s,22}$. The spectra below $T_{s,18}$ are dominated by a CH_3 symmetric stretch at 2880 cm^{-1} and a CH_3 Fermi resonance at 2940 cm^{-1}. The absence or weak contribution of the CH_3 asymmetric peak at 2955−65 cm^{-1} indicates that the molecules are oriented with the C−C−*C* axis parallel to the surface normal.[12] To obtain quantitative information, we have fitted the spectra with the following Lorentzian equation:[1]

$$I(\mathrm{SFG}) \propto \left|\chi_{\mathrm{eff,NR}} + \sum_q \frac{A_q}{\omega_{\mathrm{IR}} - \omega_q - i\Gamma_q}\right|^2 \qquad (1)$$

where A_q, Γ_q, and ω_q are the strength, damping constant, and angular frequency of a single resonant vibration, respectively. $\chi_{\mathrm{eff,NR}}$ is the nonresonant part of the signal. The magnitude of $A_q(\mathrm{r}+)/A_q(\mathrm{r}-)$ of CH_3 groups is related to the average orientation of the CH_3 groups with respect to the surface normal. The values of $A_q(\mathrm{r}+)/A_q(\mathrm{r}-)$ are similar above and below $T_{s,18}$, indicating that the average orientation of the methyl groups has not changed after the first drop in SFG intensity in the heating cycle (transition at low temperature). Hence, the drop in SFG intensity after the transition at low temperature implies that the number of ordered surface side chains has decreased abruptly. This clearly indicates the presence of two independent phases on the surface. One could perhaps argue that the ordered C22 side chains are mixed with disordered C18 side chains. However, this is not possible due to the high-energy penalty at the interface between the ordered C22 and disordered C18. The surface tension measurements indicate that there is a change in entropy and energy and hysteresis in the cooling cycle during the surface ordering transition. These results cannot be explained without the interactions with neighboring ordered chains and the existence of independent ordered C22 phase on the surface. Above $T_{s,22}$ both C18 and C22 are disordered as indicated by weak SFG intensity of the CH_3 peaks.

Since the orientation of the ordered C18 and C22 chains is similar, we can directly compare the magnitude of A_q above and below the transition temperature to determine the overall concentration of C22 chains on the surface. Figure 4b shows the results for the surface concentration, ϕ_{so}, as a function of bulk concentration of C22. In addition, we have also included data points for samples with narrower polydispersity to illustrate that the surface composition is not influenced by molecular weight or PD of the polymer chain.

There are many striking differences observed in the blends of poly(*n*-alkyl acrylates) in comparison to binary blends of alkanes that also exhibits surface freezing. First, the transition temperatures of the longer side chain component is relatively independent of bulk concentration. In the case of alkanes with large differences in chain length, the transition temperature decreases rapidly with decrease in concentration of the longer chain.[7] For the similar chain length differences as the poly(*n*-alkyl acrylates) studied here, the alkane blends are miscible in the solid state. Second, the small differences in the surface energies of ordered C22 and disordered C18 result in a dramatic surface segregation of C22 chains on the surface for ϕ_b as small as 2 wt %. Finally, we observe a significant hysteresis in the cooling cycle that increases with decrease in ϕ_b, which is not observed for blends of linear alkanes.

Here we present a simple model to explain the differences between the results for poly(*n*-alkyl acrylate) blends in comparison to that observed for small molecule alkanes. In this model, the polymer chain with n_T number of side chains has an option to place n_1 side chains on the surface and the remaining side chains within the melt. Above T_s, when the C18 and C22 chains are miscible in the bulk and on the surface, we can equate the chemical potential of C22 (and C18) in the bulk to that on the surface. The surface tension of the blend above T_s is given by the following equation (the details are provided as Supporting Information):

$$\gamma = \frac{kT}{an_1} \ln\left[\frac{1}{\phi_b e^{-\gamma_{22} an_1/kT} + (1-\phi_b) e^{-\gamma_{18} an_1/kT}}\right] \qquad (2)$$

where an_1 is the surface area occupied by C22 side chains/molecule ($a \sim 20.4$ Å^2) and γ_{22} (or γ_{18}) is the surface tension of pure C22 (or C18). A value of $n_1 \approx 5$ gives a good fit to the data shown as an inset in Figure 2. We also predict that there is a small preference to place C18 side chains on the surface above T_s, and for small values of ϕ_b the surface is predominantly covered with C18 side chains (see Supporting Information).

Below T_s, the ordered C22 side chains are phase separated from the disordered C18 chains, and we have to use the solution model instead. We can determine the surface transition temperature of the C22 phase as a function of ϕ_b after equating the chemical potential of C22 chain in the ordered phase to the C22 chain in the bulk liquid.

$$T_s = an_1(\gamma_{22}(T_s) - \gamma(T_s))/(k \ln(\phi_b)) \qquad (3)$$

$n_1 \approx n_T \approx 100$ provides a reasonable fit for the dependence of $T_{s,22}$ on ϕ_b (shown as a solid line in the inset in Figure 3). As a comparison, we have also shown the fit for $n_1 = 1$, which is expected for binary alkane blends with large differences in chain length. The large values of n_1 reduces the dependence of $T_{s,22}$ on ϕ_b, as observed for poly(*n*-alkyl acrylate) blends.

It is interesting to note that we predict that n_1 increases sharply upon cooling below the surface ordering temperature. This explains why surface transitions upon heating are sharp even at such low volume fraction of C22 chains. The order-to-disorder transition will only involve moving the C22 side chains from the surface to the near vicinity below the surface. On the other hand, cooling requires a nucleation event which is more and more unlikely at such low concentration of C22 chains in the bulk. This is the reason the hysteresis increases with decrease in ϕ_b. There are currently no theoretical models to predict the total concentration of C22 chains on the surface for phase-separated systems. This requires the knowledge of energy penalties due to grain boundaries. However, we postulate that the small differences in surface tension multiplied by large n_1 may explain the reasons for such high overall concentration of ordered C22 chains on the surface at such low values of ϕ_b.

In summary, we have for the first time studied the surface segregation in binary blends of polymers that differ in the length of the side chains. The surface segregation of C22 chains is driven by surface freezing and adding a small amount of C22 (>2 wt %) is sufficient to cover the surface with C22 below $T_{s,22}$. Below the surface ordering temperature, we predict that the polymer chains with longer side chains undergo a sharp transition to a flattened conformation with almost all the side chains/molecule participating in the surface-ordered phase. Neutron reflectivity experiments are in progress to directly confirm these predictions. The side-chain acrylates are used as smart adhesives, seed coatings, adhesive tapes, nucleating agents, and bandages.[13,14] Blending a small quantity of large side-chain component offers an unique opportunity to modify the static and dynamic surface tension for these applications.

CDV

Acknowledgment. We acknowledge funding from NSF (DMR-0512156) and L.H.'s research experience for undergraduates (DMR-0353746) and Petroleum Research Fund (40690-AC7). We also thank Professor Gujrati for helpful discussions.

Supporting Information Available: The bulk and surface thermodynamic model. This material is available free of charge via the Internet at http://pubs.acs.org.

References and Notes

(1) Gautam, K. S.; Dhinojwala, A. *Phys. Rev. Lett.* **2002**, *88*, 145501/1−4.
(2) Gautam, K. S.; Kumar, S.; Wermeille, D.; Robinson, D.; Dhinojwala, A. *Phys. Rev. Lett.* **2003**, *90*, 215501/1−4.
(3) Prasad, S.; Hanne, L.; Dhinojwala, A. *Macromolecules* **2005**, *38*, 2541−2543.
(4) Dosch, H. *Critical Phenomena at Surfaces & Interfaces*, 1st ed.; Springer-Verlag: Berlin, 1992.
(5) Ocko, B. M.; Wu, X. Z.; Sirota, E. B.; Sinha, S. K.; Gang, O.; Deutsch, M. *Phys. Rev. E* **1997**, *55*, 3164−3182.
(6) Gang, O.; Wu, X. Z.; Ocko, B. M.; Sirota, E. B.; Deutsch, M. *Phys. Rev. E* **1998**, *58*, 6086−6100.
(7) Sloutskin, E.; Wu, X. Z.; Peterson, T. B.; Gang, O.; Ocko, B. M.; Sirota, E. B.; Deutsch, M. *Phys. Rev. E* **2003**, *68*, 031605/1−031605/13.
(8) Gautam, K. S.; Schwab, A. D.; Dhinojwala, A.; Zhang, D.; Dougal, S. M.; Yeganeh, M. S. *Phys. Rev. Lett.* **2000**, *85*, 3854−3857.
(9) The spectra taken with the same setup have broad wavenumber (fwhm ≈ 20 cm^{-1}) resolution. For narrow wavenumber (fwhm < 5 cm^{-1}) resolution[15] we have used a SpectraPro-500i monochromator in front of the detector.
(10) Synthesis of monomer was done by reacting alcohol of appropriate alkyl chain length with acryloyl chloride. Polymerization was performed in benzene solvent at 333 K with azobis(isobutyronitrile) (AIBN) as initiator.
(11) $\ln(\phi_s/\phi_b) = A(\gamma - \gamma_{22})/kT$.[16] A is the area occupied by a molecule on the surface, and γ_{22} is the surface tension of C22 homopolymer.
(12) Gautam, K. S.; Dhinojwala, A. *Macromolecules* **2001**, *34*, 1137−1139.
(13) Kinning, D. J. *J. Adhes.* **1997**, *60*, 249−274.
(14) De Crevoisier, G.; Fabre, P.; Corpart, J.-M.; Leibler, L. *Science* **1999**, *285*, 1246−1249.
(15) Harp, G. P.; Rangwalla, H.; Yeganeh, M. S.; Dhinojwala, A. *J. Am. Chem. Soc.* **2003**, *125*, 11283−11290.
(16) Defay, R.; Prigogine, I. *Surface Tension and Adsorption;* John Wiley: New York, 1966.

MA061266E